Counterion Distribution around DNA Probed by Solution X-Ray Scattering

R. Das,[1,2] T. T. Mills,[3] L. W. Kwok,[3] G. S. Maskel,[3] I. S. Millett,[4] S. Doniach,[2] K. D. Finkelstein,[5] D. Herschlag,[1,4] and L. Pollack[3]

[1]Department of Biochemistry, Stanford University, Stanford, California 94305, USA
[2]Department of Physics, Stanford University, Stanford, California 94305, USA
[3]School of Applied and Engineering Physics, Cornell University, Ithaca, New York 14853, USA
[4]Department of Chemistry, Stanford University, Stanford, California 94305, USA
[5]Cornell High Energy Synchrotron Source (CHESS), Cornell University, Ithaca, New York 14853, USA

Counterion atmospheres condensed onto charged biopolymers strongly affect their physical properties and biological functions, but have been difficult to quantify experimentally. Here, monovalent and divalent counterion atmospheres around DNA double helices in solution are probed using small-angle x-ray scattering techniques. Modulation of the ion scattering factors by anomalous (resonant) x-ray scattering and by interchanging ion identities yields direct measurements of the scattering signal due to the spatial correlation of surrounding ions to the DNA. The quality of the data permit, for the first time, quantitative tests of extended counterion distributions calculated from atomic-scale models of biologically relevant molecules.

PACS numbers: 87.14.Gg, 61.10.Eq, 87.15.–v

The intricate folding and biological functions of the highly negatively charged biopolymers RNA and DNA are intimately coupled to the positive counterions that neutralize them [1]. Thus, a detailed understanding of the counterion environment is essential for a full description of all nucleic acid systems in biology. However, the long range of electrostatic forces and the many degrees of freedom in the counterion cloud render experimental and theoretical characterization of counterion distributions a formidable challenge [2].

Early model calculations for uniformly charged rods [3] and for lines of discrete charges [4], critically compared in [5], indicated that counterions condense around a nucleic acid chain in a tightly bound layer. It is now possible to quantitatively estimate the distributions of counterions around realistic models of nucleic acids. In particular, the speed of numerical implementation of the nonlinear Poisson-Boltzmann (NLPB) model allows for fine-grained mapping of counterions around large biomolecules at atomic-scale resolution [6,7]. Despite its popularity in biophysical studies, the NLPB approach is not exact, as it ignores the finite sizes of ions and ion-ion correlations. Fortuitously, an approximate cancellation between these two complex factors results in reasonable, though not exact, agreement of ion concentration profiles predicted from the NLPB model and from more sophisticated calculations, such as Monte Carlo simulations, for monovalent and divalent counterions around DNA [8]. It is thus not surprising that the NLPB predictions of counterion distributions are in qualitative agreement with previous experiments [2,5,9,10].

Recent theoretical work suggests, however, that enhanced counterion correlations for more strongly charged polyelectrolytes and counterions can lead to dramatic phenomena ranging from an effective reversal of the DNA's charge to *attraction* between usually repelling double helices [11]. These effects cannot be described in the basic NLPB approach, but may be integral to the biological behavior of nucleic acids, including RNA folding [12] and DNA collapse into toroidal aggregates [13]. A prerequisite to understanding these processes is a knowledge of the ion atmosphere's properties under conditions favorable for counterion-correlation-induced attraction.

Unfortunately, most experimental approaches for studying ion atmospheres provide either "global" numbers of certain types of bound ions or "local" estimates of electrostatic potential near the nucleic acid [6]. Few data are available, however, that constrain the spatial extent of counterion atmospheres around nucleic acids. Quantitative interpretations of ion distributions based on quadrupolar cation NMR relaxation rates [2], on force measurements in DNA gels [9], and on energy transfer between luminescent ions [10] are difficult due to uncertainties in modeling these complex processes. In this Letter, we present a new tool to understand the ions, based on small-angle x-ray scattering (SAXS) measurements. This proof-of-principle study investigates counterions condensed onto a 25-base-pair DNA double helix. For the first time, a quantitative comparison of the full theoretical ion distributions predicted from atomic-scale models to experimental data has been carried out.

The experimental background for this scattering technique has been developed by several groups. It has been recognized since early solution scattering work on DNA [14] that the measured scattering intensity profile is sensitive to the shape of the counterion atmosphere, although deconvolving the ion contribution from the overall profile is challenging. Recent neutron scattering studies by van der Maarel and collaborators have successfully isolated

the spatial correlation signal between DNA and ion scattering for samples of long DNA fragments using D_2O/H_2O contrast matching [15]. However, quantitative comparison to atomic-scale models has proven to be challenging due to the difficulty of accounting for the contrasts of polyelectrolyte, ions, and bound solvent simultaneously (cf. [16]). An alternative approach, anomalous small-angle scattering (ASAXS) [17], varies the contrast of counterions at energies close to their atomic absorption edge, and has been qualitatively used to study heavy ions around a light model polyelectrolyte [18].

We have now applied SAXS and ASAXS to quantitatively characterize the ion atmospheres in a biologically relevant system: a nucleic acid in solution. The 25-deoxynucleotide single strand *GCATCTGGGCTATAAAA GGGCGTCG* and its complement were chemically synthesized (Operon) and purified to produce aqueous DNA stocks with neutralizing ammonium counterions and no added salt. Sodium, rubidium, magnesium, or strontium solutions (with acetate co-ions) were mixed with preannealed DNA double-helix stocks for final counterion concentrations of 0.4 M, and DNA concentrations of 0.5 mM (monovalent samples) and 1.7 mM (divalent samples). The double helix is stable and fully charged under these conditions (pH > 6, 22 °C). Scattering curves with DNA concentrations down to 0.1 mM, acquired at the Stanford Synchrotron Radiation Laboratory (SSRL), display no concentration dependence and indicate that interparticle interference effects are negligible for these measurements, in contrast to [15,19].

SAXS data were acquired at the C1 station of the Cornell High Energy Synchrotron Source (CHESS) [20]. Samples with monovalent counterions were probed with x-ray energies of 15.10 and 15.19 keV (Rb K edge); samples with divalent counterions, at 16.02 and 16.10 keV (Sr K edge). The anomalous scattering factor differences ($\Delta f'$) between the pairs of energies are -2.6 ± 0.5 electrons per Rb ion and -2.8 ± 0.5 electrons per Sr ion, determined by a Kramers-Kronig transform of measured x-ray transmission [21]. After subtraction of background profiles taken on solutions with matching total ion concentration, scattering profiles were divided by DNA concentration and by transmitted beam intensity. To correct for isotropic fluorescence in measurements at anomalous edge x-ray energies, a uniform offset has been applied to those profiles to match off-edge curves at the highest scattering angles, as in other ASAXS studies [17,18].

Our predictions of the scattering profile $I(s)$ [with $s = 2\sin(\theta/2)/\lambda$; θ is the scattering angle] include scattering from the DNA itself and from correlations between DNA and surrounding ions [17]:

$$I(s) \propto b_D^2 I_{DD}(s) + 2b_D b_I n_I I_{DI}(s), \quad (1)$$

where b_D and b_I are scattering factors for the hydrated DNA and ion, respectively; and n_I is the number of ions condensed onto each DNA. The component terms $I_{ij}(s)$

(here normalized to unity at $s = 0$) are related by the standard Debye formula to spatial correlation functions $P_{ij}(r)$ of pairwise distances r, weighted by the electron densities of the hydrated solutes i and j relative to the bulk solvent [22], and were calculated in MATLAB routines (Mathworks, Inc.). Inclusion of scattering terms due to ion-ion correlations and to exclusion of acetate co-ions from DNA has a negligible effect on the fits below. The calculations employed atomic coordinates for the DNA double helix [23], and theoretical counterion distributions predicted with the program DELPHI [6,7]. In the DNA model, atoms (C, N, O, and P) were weighted by solvent-subtracted scattering factors used in the CRYSOL program [24]. The scattering factors b_I were determined empirically (see below).

Figure 1 displays the SAXS profiles for the 25-base-pair double helix with four types of counterions. First, the enhanced scattering of ion atmospheres composed of "heavy" counterions relative to atmospheres of lighter ions is reflected in the increased overall intensity of the former profiles (Rb$^+$ vs Na$^+$; Sr^{2+} vs Mg^{2+}). Second, all DNA experimental curves decrease more steeply than the predicted profile for the double helix alone: The DNA scatters as if it is a "fatter" molecule than a bare helix. Similar effects have been noted in previous studies of longer DNAs [14,19] and other polyelectrolytes [25], and have been qualitatively explained with simplified rod models of the polymers and their ion clouds. Here, atomic-scale calculations of DNA-counterion scattering, with optimized counterion scattering factors (see below), result in exceptional fits (solid lines, Fig. 1) to experimental curves that are significant improvements over previously published comparisons.
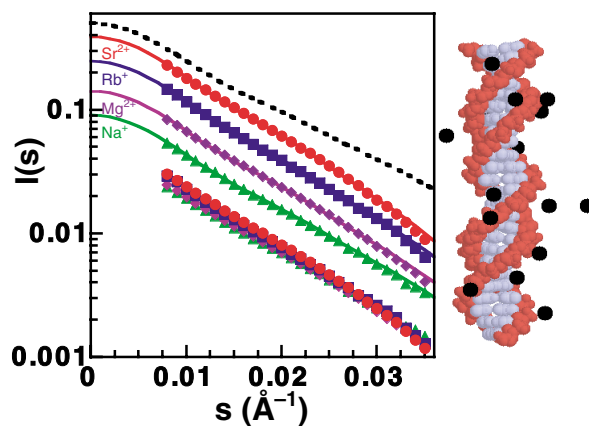

FIG. 1 (color online). X-ray scattering profiles for DNA, in the presence of 0.4 M Na$^+$ (triangles), Mg^{2+} (diamonds), Rb$^+$ (squares), and Sr^{2+} (circles) counterions. Actual curves (bottom) are shown, as well as offset curves (top), to aid visual comparison with calculations for DNA without modeled counterions (dashed line, arbitrary normalization) and with NLPB ion atmospheres (solid lines). To the right is shown a 25-base-pair DNA double helix in the presence of divalent cations (black spheres), distributed according to an NLPB calculation.

More direct evidence for the condensation of Rb^+ and Sr^{2+} counterions to DNA double helices was obtained by tuning the x-ray energy to the appropriate absorption edge to suppress the ion scattering. Indeed, this effect is clearly seen in the experimental anomalous scattering profiles (Fig. 2). Control samples with Na^+ (Mg^{2+}) counterions display no detectable difference in scattering at the Rb (Sr) anomalous edge (divalent data shown). Further anomalous scattering measurements with DNA in counterion concentrations of 50:50 mixtures of Rb^+:Na^+ (Sr^{2+}:Mg^{2+}) exhibit half the suppression seen for the DNA in pure Rb^+ (Sr^{2+}) samples (data not shown). Therefore, not only is there a counterion atmosphere condensed onto the DNA, but also a common theoretical assumption is supported: Counterions of the same valence are interchangeable within the atmosphere.

In Fig. 3, difference curves between the scattering profiles measured at and below the anomalous absorption edges are compared to NLPB calculations of the DNA-ion correlation signal. The curves, scaled to match the areas of the theoretical and experimental profiles, display good shape agreement. In addition, the relative strength at zero scattering angle of Rb^+ and Sr^{2+} anomalous signals (divided by $\Delta f'$) yields the ratio of the total number of Rb^+ to Sr^{2+} cations bound to the DNA in the two samples. The result, 2.0 ± 0.3, based on the ratio of the anomalous difference signals extrapolated to zero scattering angle, clearly demonstrates that more monovalent cations than divalent cations are required to neutralize the DNA. This

appears to be the first experimental verification of such a clearly basic theoretical prediction.

An independent estimate of the DNA-ion correlation signal can be obtained by subtracting scattering curves taken in separate DNA samples with counterions of the same valence but different scattering power, similar to "heavy-atom replacement" techniques in crystallography [26]. This procedure assumes that diffusely bound counterions of the same valence are interchangeable, as validated by the ASAXS measurements above. The shapes of the Rb^+–Na^+ and Sr^{2+}–Mg^{2+} difference curves agree well with the corresponding Rb^+ and Sr^{2+} anomalous difference curves (Fig. 3). Furthermore, the scaling required to match the pairs of curves provides absolute calibrations of the DNA and counterion scattering factors, whose physical interpretation we discuss next.

The 25-base-pair DNA and each monovalent ion have scattering factors of 2600 ± 500 (DNA), 7 ± 2 (Na^+), and 16 ± 3 electrons (Rb^+) at 15.10 keV, less than their scattering in vacuum (Z numbers of 8500, 10, and 36, respectively) due to low contrast with the water background. The empirical number for DNA agrees well with the calculated solvent-subtracted value of 3200 electrons from the CRYSOL program [24]. In striking contrast, the divalent ions contribute 22 ± 4 (Mg^{2+}) and 41 ± 8 (Sr^{2+}) electrons at 16.02 keV, dramatic enhancements over vacuum values (10 and 36 electrons, respectively). A variety of experimental measurements, including ion viscosity, water entropy, and densitometric data [27,28], have
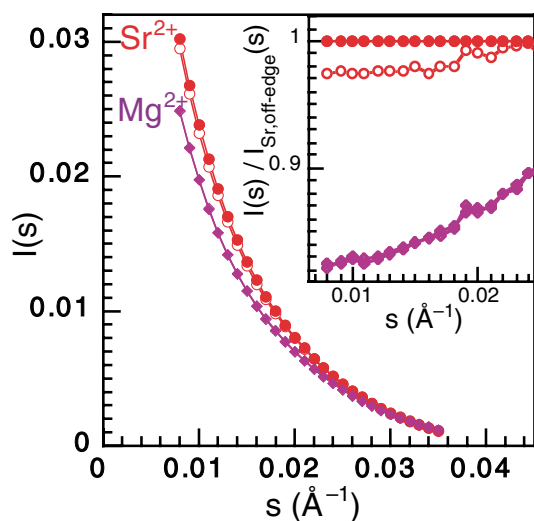

FIG. 2 (color online).   Direct evidence for counterion condensation onto DNA. Scattering in the presence of Sr^{2+} counterions probed with x-ray energies off (solid circles) and on (open circles) the Sr anomalous edge; and "control" measurements on DNA with Mg^{2+} counterions probed off and on the Sr edge (solid and open diamonds, indistinguishable). Inset: Magnification of curves, each divided by the off-edge Sr^{2+} profile to aid visual comparison. Error bars are smaller than symbols.
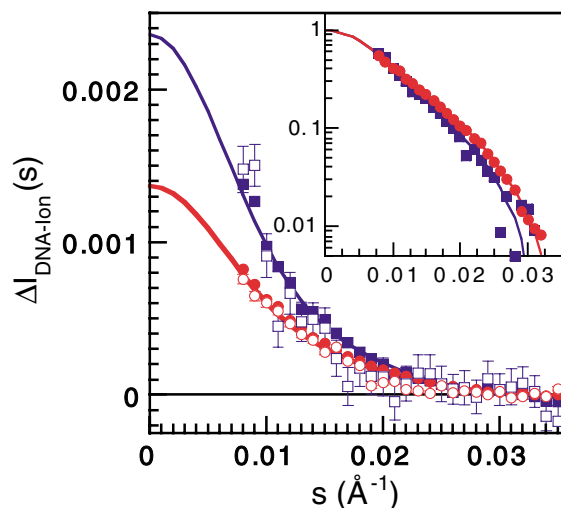

FIG. 3 (color online).   DNA-counterion correlation signals. Differences between profiles taken off and on anomalous edge for DNA with Rb^+ (open squares) and Sr^{2+} (open circles), compared to the following: NLPB predictions for monovalent and divalent ion atmospheres (lines); Rb^+–Na^+ difference curve (solid squares); and Sr^{2+}–Mg^{2+} difference curve (solid circles). Inset: Shape comparison (log scale) of same NLPB, Rb^+–Na^+, and Sr^{2+}–Mg^{2+} curves, now renormalized by the intensity extrapolated to zero scattering angle with a Porod fit $[\log(sI/I_0) \propto -s^2]$ of the data at $s = 0.01$–0.02 Å^{-1} [14].

suggested that the "chaotropic" monovalent ions exclude and disorder surrounding water, whereas "kosmotropic" divalent ions have dense, ordered hydration shells. The higher x-ray scattering factors of divalent ions relative to their monovalent counterparts of the same atomic number provide clear evidence of these hydration effects.

Finally, the excellent signal-to-noise of the Rb^+–Na^+ and Sr^{2+}–Mg^{2+} difference curves, compared to the anomalous difference data, allows for a precise test of the predicted atmosphere shapes, which have been difficult to investigate quantitatively until now. The thickness of the condensed monovalent counterion layer is expected to be roughly twice that of the divalent atmosphere, e.g., the screening lengths are 4.9 and 2.9 Å, respectively. The predicted difference in layer thickness, although small compared to the ~12 Å DNA radius, is clearly reflected in the enhanced steepness of the monovalent DNA-ion correlation data relative to the divalent data (see Fig. 3 inset). Furthermore, the data are in excellent agreement with the NLPB predictions.

In conclusion, we have used SAXS and, for the first time, anomalous SAXS to experimentally probe the biologically essential but usually hidden partner of nucleic acids, the counterion atmosphere. Inclusion of scattering from the hydrated counterions proves necessary for understanding the SAXS profiles of 25-base-pair DNA double helices in solution. Modulating the ion scattering factor with ASAXS techniques provides an exceptionally direct demonstration of the condensation of counterions onto DNA, with measurements carried out on a single sample. Furthermore, subtracting SAXS profiles with interchanged counterions of the same valence but different scattering power yields independent measurements of the DNA-ion correlation signals.

We find unprecedented, quantitative agreement between the data and atomic-scale NLPB calculations, validating this popular biophysical approach for these simple DNAs with monovalent and divalent ions, and demonstrating the application of a powerful method for the further exploration of a wide variety of DNA-ion systems under biological conditions. Future studies will extend beyond the regime of charge compensation where NLPB is valid. When applied to systems with higher charge density and higher valence counterions, ASAXS techniques should provide direct tests of charge inversion and latticelike ion ordering in DNA condensates [11], recently predicted from theories taking into account strong counterion correlations.

[1] A. L. Feig and O. C. Uhlenbeck, in *The RNA World*, edited by R. F. Gesteland, T. R. Cech, and J. F. Atkins (Cold Spring Harbor Laboratory Press, New York, 1999), pp. 287–319.

[2] C. F. Anderson and M. T. Record, Jr., Annu. Rev. Biophys. Biophys. Chem. **19**, 423 (1990).

[3] R. M. Fuoss, A. Katchalsky, and S. Lifson, Proc. Natl. Acad. Sci. U.S.A. **37**, 579 (1951).

[4] G. S. Manning, J. Chem. Phys. **51**, 924 (1969).

[5] P. L. Hansen, R. Podgornik, and V. A. Parsegian, Phys. Rev. E **64**, 021907 (2001).

[6] V. K. Misra and D. E. Draper, J. Mol. Biol. **299**, 813 (2000), and references therein; also, J. L. Hecht *et al.*, J. Phys. Chem. **99**, 7782 (1995).

[7] S. W. Chen and B. Honig, J. Phys. Chem. B **101**, 9113 (1997).

[8] G. R. Pack, L. Wong, and G. Lamm, Biopolymers **49**, 575 (1999); C. N. Patra and A. Yethiraj, J. Phys. Chem. B **103**, 6080 (2000); M. Deserno, C. Holm, and S. May, Macromolecules **33**, 199 (2000).

[9] R. Podgornik, D. C. Rau, and V. A. Parsegian, Macromolecules **22**, 1780 (1989).

[10] T. G. Wensel *et al.*, Proc. Natl. Acad. Sci. U.S.A. **83**, 3267 (1986).

[11] A. Yu. Grosberg, T. T. Nguyen, and B. I. Shklovskii, Rev. Mod. Phys. **74**, 329 (2002); N. Grønbech-Jensen *et al.*, Phys. Rev. Lett. **78**, 2477 (1997).

[12] R. Russell *et al.*, Nat. Struct. Biol. **7**, 367 (2000); S. L. Heilman-Miller, D. Thirumalai, and S. A. Woodson, J. Mol. Biol. **306**, 1157 (2001); R. Russell *et al.*, Proc. Natl. Acad. Sci. U.S.A. **99**, 4266 (2002).

[13] V. A. Bloomfield, Biopolymers **44**, 269 (1997).

[14] V. Luzzati, A. Nicolaieff, and F. Masson, J. Mol. Biol. **3**, 185 (1961); V. Luzzati *et al.*, Biopolymers **5**, 491 (1967); S. Bram and W. W. Beeman, J. Mol. Biol. **55**, 311 (1971).

[15] S. S. Zakharova *et al.*, J. Chem. Phys. **111**, 10706 (1999).

[16] G. Zaccai and S.-Y. Xian, Biochemistry **27**, 1316 (1988).

[17] A. Naudon, in *Modern Aspects of Small-Angle Scattering*, edited by H. Brumberger (Kluwer, Netherlands, 1995), p. 203.

[18] B. Guilleaume *et al.*, Colloid Polym. Sci. **279**, 829 (2001); ASAXS has also recently been applied to condensed DNA fibers [N. O. Kozlova and H. H. Strey (unpublished)].

[19] S.-L. Chang *et al.*, J. Phys. Chem. **94**, 8025 (1990).

[20] K. D. Finkelstein, P. M. Abbamonte, and V. O. Kostroun, Proc. SPIE **4783**, 139 (2002).

[21] J. J. Hoyt, D. de Fontaine, and W. K. Warburton, J. Appl. Crystallogr. **17**, 344 (1984).

[22] S. Doniach, Chem. Rev. **101**, 1763 (2001).

[23] Y. Liu and D. L. Beveridge, J. Biomol. Struct. Dyn. **18**, 505 (2001).

[24] D. Svergun, C. Barberato, and M. H. J. Koch, J. Appl. Crystallogr. **28**, 768 (1995).

[25] B. Guilleaume *et al.*, J. Phys. Condens. Matter **12**, A245 (2000); C. F. Wu *et al.*, Phys. Rev. Lett. **61**, 645 (1988); W. Essafi, F. Lafuma, and C. Williams, Eur. Phys. J. B **9**, 261 (1999).

[26] V. Tereshko *et al.*, Nucleic Acids Res, **29**, 1208 (2001).

[27] K. D. Collins, Biophys. J. **72**, 65 (1997).

[28] F. J. Millero, Chem. Rev. **71**, 147 (1971).